Challenge Journal of CONCRETE RESEARCH LETTERS

Research Article

Effect of bacteria and fibers on the mechanical and structural behavior of self-healing fibrous concrete

Mina Medhat Youssef [a,*], Alaa Ali Bashandy [a], Rateb Nabil Abbas [b], Amal Abdel Hady Nasser [a]

[a] Department of Civil Engineering, Menoufia University, 32511 Shebin ElKoum, Menofia, Egypt

[b] Department of Microbial Biotechnology, Genetic Engineering and Biotechnology Research Institute, University of Sadat City, 32 897 Sadat City, Egypt

ABSTRACT

The incorporation of bacteria into concrete has emerged as a promising strategy to enhance mechanical performance. This study presents a comprehensive experimental and numerical investigation into the behavior of fibrous concrete incorporating two bacterial strains—Bacillus megaterium (BM) and W1 at a dosage of 0.25% of cement weight, combined with either steel or polypropylene fibers. A multiscale experimental program was carried out, including compressive, tensile, and flexural tests, along with structural slab evaluation and analytical validation. Results revealed significant strength enhancements due to the steel fiber–BM combination, with compressive strength improvements of 42%, 52%, and 31% at 7, 28, and 90 days, respectively, compared to the control. Using polypropylene fiber–W1 mixes, recorded tensile strength gains reached nearly 19%. Flexural strength increased by up to 30% in 90 days, confirming the synergistic effect of fiber crack-bridging and bacterial precipitation. Structural performance was further assessed through four-point bending tests on reinforced slabs (1.0 m × 0.5 m × 0.05 m), where bacterial–fibrous concretes exhibited superior ductility and load capacity compared to the control. Reinforcing with steel plates proved more effective than glass fiber laminates, achieving 15–17% higher ultimate loads. A finite element model developed in Abaqus/CAE using the Concrete Damaged Plasticity model accurately replicated the experimental load–deflection responses, validating the proposed approach. Overall, the results demonstrate that integrating bacteria with fibers and external reinforcement can substantially enhance both material- and structural-scale performance, highlighting its potential for durable, high-performance concrete applications. These findings underline the potential of fibrous concrete as a sustainable, durable, and cost-effective solution for future structural applications.

ARTICLE INFO

Article history:

Received – October 6, 2025
Revision requested – November 10, 2025
Revision received – December 5, 2025
Accepted – December 11, 2025

Keywords:

Bacteria
Polypropylene fiber
Steel fiber
Glass fiber
Fibrous concrete
Self-healing concrete
Steel plates

Citation: Youssef MM, Bashandy AA, Abbas RN, Nasser AAH (2026). Effect of bacteria and fibers on the mechanical and structural behavior of self-healing fibrous concrete. *Challenge Journal of Concrete Research Letters*, 17(1), 13–29.

1. Introduction

For decades, engineers and scientists have strived to extend the service life of structures and components through research and innovation. One promising strategy is the development of bio-enhanced composite materials (Igbokwe et al. 2022). Concrete remains the most widely used material in the global construction industry due to its affordability, durability, high compressive strength, thermal mass, and versatility. However, concrete exhibits low tensile strength and high compressive strength, making cracking inevitable (Puranik et al. 2019). Once cracks appear, the lifespan of concrete structures can be significantly reduced. Although various crack repair methods exist, they are often costly and time-consuming. A major concern is the increased risk of

* *Corresponding author.* E-mail address: mina_medhat@sh-eng.menofia.edu.eg (M. M. Youssef)

ISSN: 2548-0928 / DOI: https://doi.org/10.20528/cjcrl.2026.01.002

structural failure caused by cracks under service conditions, which may result from factors such as general loading, drying shrinkage, creep, and thermal stresses (Ganesh et al. 2020). These cracks create pathways for aggressive chemicals and fluids to penetrate, leading to deterioration of the embedded reinforcement or cement matrix. Since cracking in concrete structures during their service life is unavoidable, enhancing material performance and potentially facilitating crack closure solutions has become essential. Self-healing involves the formation of solid substances within cracks through chemical or physical reactions, thereby blocking the ingress of harmful agents (Ji et al. 2020). Today, concrete continues to dominate infrastructure construction worldwide is provided by the works of Mutitu (2009) and Wachira et al. (2019).

In recent years, self-healing concrete has emerged as a promising innovation in the construction industry (de Brito and Kurda 2021). Concrete structures are often exposed to harsh environmental conditions that compromise durability, leading to expansion, cracking, and potential structural failures. These issues not only reduce service life but also increase maintenance costs and safety risks. To address these challenges, researchers have focused on developing smart concrete solutions that incorporate self-healing technologies to enhance resilience and longevity. Self-healing mechanisms are particularly beneficial in inaccessible or hazardous environments, where conventional repair methods are impractical. By autonomously sealing cracks and preventing the ingress of harmful agents, self-healing concrete offers a sustainable approach to maintaining structural integrity under demanding conditions (Helal et al. 2024). Later research focuses on biotechnology and civil engineering aspects of developing self-healing concrete. The global demand for buildings has driven the widespread use of concrete since the era of ancient Rome (Ryparova et al. 2021). However, conventional repair methods present several drawbacks, including operational limitations during reconstruction, mismatched thermal expansion between the base matrix and repair material, and potential environmental hazards (Griño et al. 2023).

The combination of fibers and bacteria accelerates the self-repair process in concrete. Bacteria such as Bacillus subtilis and Bacillus sphaericus produce calcium carbonate ($CaCO_3$) which fills the cracks, while fibers help in reducing crack width and providing a scaffold for the deposition of healing materials (Su et al. 2021).

The development of bio-based self-healing concrete seeks to minimize durability problems caused by cracking. Consequently, scientists are exploring various self-repair techniques (Ahmed et al. 2021; Mohammed et al. 2020; Ryparova et al. 2021; Xu et al. 2020). Innovative bio-materials that enhance calcite precipitation have been designed to facilitate the self-healing of cracks (İsar et al. 2023; Nasser et al. 2022; Nimafar et al. 2023; Ryparova et al. 2021; Singh et al. 2023). Incorporating specific microorganisms into cementitious materials is recognized as a cost-efficient and environmentally friendly approach for repairing micro-cracks. The microbial self-healing mechanism presents a highly promising solution, as it enables continuous crack healing, resulting in significant enhancement of the physico-mechanical properties of bio-concrete (Ahmed et al. 2021; Mohammed et al. 2020; Ryparova et al. 2021; Saridhe and Selvaraj 2021). Microbial-induced calcite precipitation (MICP) is a biological process in which specific microorganisms facilitate the formation of calcite through various mechanisms (Ryparova et al. 2021; Sadeghpour and Baradaran 2023). As a result, it enhances the mechanical and structural properties of concrete structures without the need for expensive or time-intensive repairs. The inclusion of fibers and bacteria improves the compressive strength, tensile strength, and flexural strength of concrete. For instance, the use of natural fibers like flax and coir has shown substantial improvements in crack-healing and compressive strength (Rauf et al. 2020). The bio-induced precipitation of calcite, driven by microbial metabolic activity within the concrete matrix, enhances material durability and represents a natural self-healing mechanism (Ahmed et al. 2021; Rossi et al. 2021; Roy et al. 2021). Microbial self-healing in bio-concrete typically involves two metabolic pathways: one through urea hydrolysis by Ureolytic bacteria and the other through respiration by non-Ureolytic bacteria (Rossi et al. 2021; Ryparova et al. 2021; Xu et al. 2020). In this context, Ureolytic bacteria like Bacillus megaterium and W1 have attracted significant attention in bio-cementation methods. Both bacterial strains are commonly found in soil and aquatic environments. They are Gram-positive, aerobic, rod-shaped, non-pathogenic organisms that exhibit urease activity and can tolerate highly alkaline conditions (Bakr et al. 2024; Su et al. 2021; Islam and Waseem 2023; Han et al. 2020). Certain bacterial species can hydrolyze urea into carbonate ions and ammonium (Nasser et al. 2022; Wang et al. 2023). The resulting ammonia increases the pH, which promotes calcite precipitation within micro-cracks, effectively sealing them (Tang and Xu 2021). Utilizing sustainable, eco-friendly biomaterials in construction offers an alternative to conventional chemical-based methods, reducing potential environmental and health risks (Ryparova et al. 2021; Nasser et al. 2022). In line with this approach, the present study aims to develop a novel sustainable bio-concrete incorporating ureolytic bacteria. The research evaluates the physical and mechanical properties of the bio-concrete at different curing stages and highlights the quantifiable improvements in compressive, tensile, and flexural performance attributed to the inclusion of bacteria and fibers. (Ahmed et al. 2021; Nasser et al. 2022; Zahran et al. 2014).Despite several studies on self-healing concrete, few investigations have compared the effects of multiple bacterial types combined with different fiber reinforcements. Moreover, limited research has addressed the correlation between mechanical properties at the material scale and structural performance. These gaps justify the current study, which aims to evaluate the combined effect of bacterial self-healing and fiber reinforcement on both material and structural behavior of concrete.

2. Research Significance

This research highlights the promising role of combining bacterial self-healing technology with fiber reinforcement in enhancing concrete performance. The research significance lies in providing a systematic understanding of the mechanical behavior and structural performance of self-healing concrete reinforced with fibers, as well as external reinforcement.

The novelties of this investigation are three points: (i) obtaining fibrous self-healing concrete using polypropylene fibers or steel fibers, (ii) a comparative study on the combined two bacterium types, Bacillus megaterium and W1, to obtain self-healing concrete, and (iii) the evaluation of the structural performance of fibrous self-healing concrete slabs. These findings will support researchers and engineers in adopting such a concrete type in construction practices. By validating these benefits, the study contributes to advancing innovative materials that align with the growing global demand for resilient and eco-friendly construction practices.

3. Experimental Program

The experimental program was designed to evaluate the mechanical performance of bio-concrete incorporating bacteria and fibers. The overall procedure is summarized in the flow chart (Fig. 1).

3.1. Materials

3.1.1. Cement

Ordinary Portland Cement (OPC, CEM I 42.5N) was used, sourced from El Sewedy Cement, Egypt. The specific Gravity is 3.15 (dimensionless). The cement complied with the requirements of the Egyptian Standard Specifications (E.S.S. 4756-1/2022 (2022)). A fixed cement content of 500 kg/m^3 was adopted for all mixes.

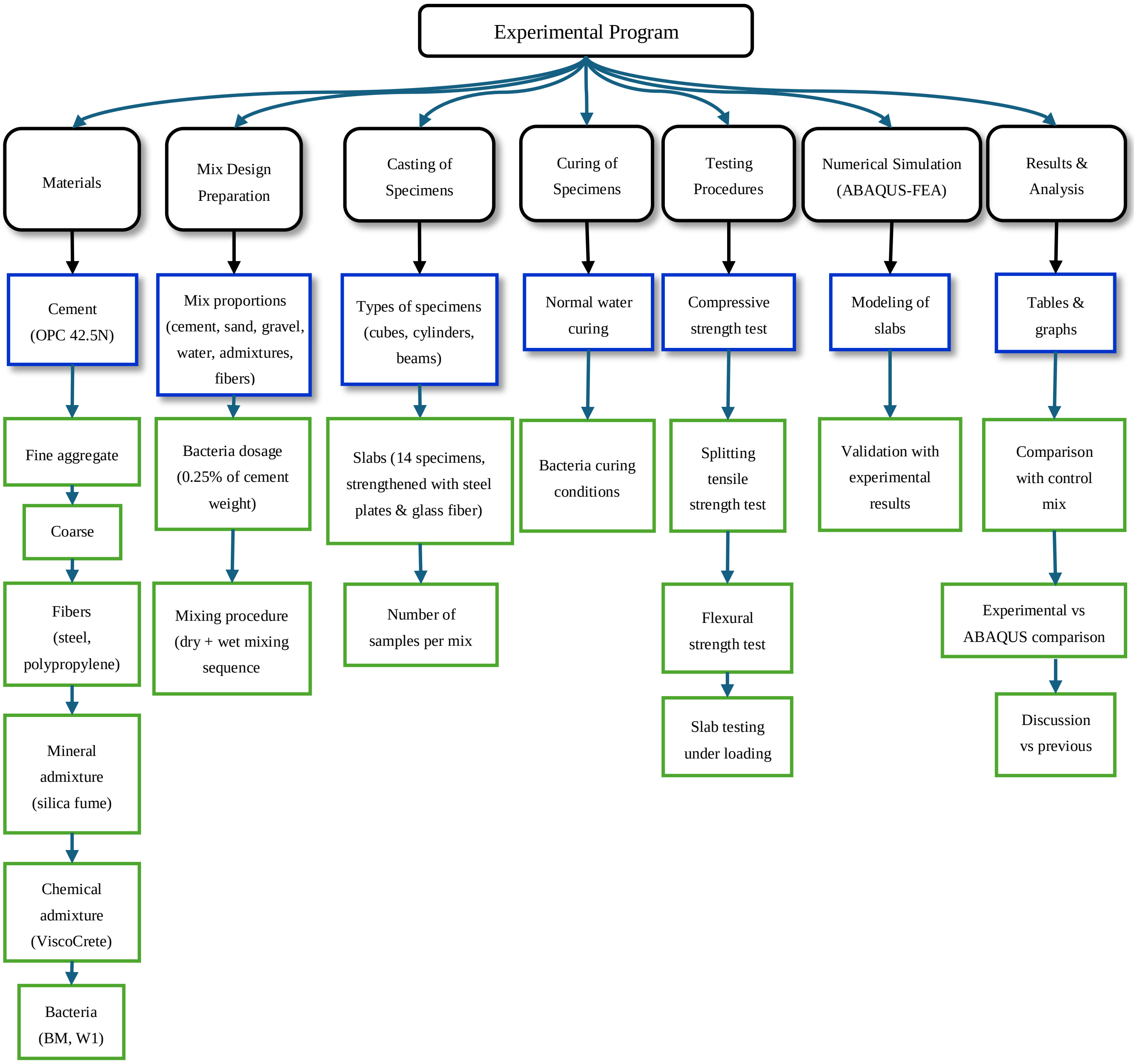

Fig. 1. Flow chart of research methodology.

3.1.2. Water

Fresh tap water, free from impurities, was used for casting and curing of all mixtures. The water-to-cement (W/C) is 0.42 for all mixes.

3.1.3. Fine aggregates

Well-graded sand was used as fine aggregate to minimize the void ratio. Standard characterization tests were conducted in accordance with ASTM procedures, including water absorption, specific gravity, and fineness modulus analysis. The results are presented in Table 1.

3.1.4. Coarse aggregates

Locally sourced crushed limestone with a maximum nominal size of 20 mm was employed as coarse aggregate. Characterization results for both fine and coarse aggregates are also summarized in Table 1.

Table 1. Physical properties of aggregate.

Physical property	Fine aggregate	Coarse aggregate
Specific gravity	2.60	2.62
Fineness modulus	2.36	4.1
Bulk density	1702 kg/m^3	1456 kg/m^3
Water absorption	0.85%	2%

3.1.5. Admixtures

Silica fume:

Silica fume (commercial product: Sika Fume, supplied by Sika Egypt) was incorporated as a supplementary cementitious material. The material consists of ultra-fine amorphous silicon dioxide particles with an average size of approximately 0.1 µm. In fresh concrete, silica fume enhances cohesion and water retention, while in hardened concrete, it chemically reacts with calcium hydroxide (free lime) released during cement hydration, forming additional calcium silicate hydrate (C–S–H) gel. This secondary hydration product densifies the microstructure and improves both strength and durability. The technical properties of the silica fume used in this study are summarized in Table 2.

Water-reducing admixture:

A high-range water-reducing admixture, Sika ViscoCrete®-3425, was used to enhance the workability of fresh concrete. This admixture is particularly suitable for producing mixes with high early strength development, significant water reduction, and superior flowability. It is chloride-free and does not contain any components that may accelerate steel reinforcement corrosion, thus making it appropriate for use in both reinforced and prestressed concrete. The main technical characteristics of Sika ViscoCrete®-3425 are provided in Table 3.

Table 2. Technical data of silica fume (obtained from the manufacturer).

Particle size (silicon dioxide)	~ 0.1 µm
Appearance / Color	Grey powder
Bulk density	300 kg/m^3
Dosage	2–10% by weight of cement (in this product) for optimum results
SiO_2	≥ 85%
Specific gravity	2.3
Specific surface area	> 20 m^2/g

Table 3. Technical data of superplasticizer used, "Sika ViscoCrete" (obtained from the manufacturer).

Base	Aqueous solution of modified polycarboxylates
Appearance/Color	Clear liquid
Density	1.08 kg/lt (ASTM C494)
pH value	4.0
Solid content	40% by weight.

3.1.6. Fibers and plates

Steel (as internal and external reinforcement):

Steel fibers (Fig. 2) with a density of 7850 kg/m^3, a length of 3 cm, and an equivalent diameter of 0.2 mm were employed. These fibers exhibit an aspect ratio of 150. The fibers were procured from the Chemical for Modern Building Company, Egypt.

Steel plates (Fig. 2) with a thickness of 2 mm and a width of 5 cm along the slab span were employed as external reinforcement. The plates were sourced from locally fabricated by a certified metal workshop in Egypt.

Polypropylene fiber (as internal reinforcement):

The properties of polypropylene are governed by factors such as crystallinity, comonomer type and proportion, molecular weight, molecular weight distribution, and isotacticity. In this study, polypropylene fibers with a diameter of 0.05 mm, a length of 12 mm, and a density of 900 kg/m^3 were incorporated into bio-concrete. These fibers exhibit an aspect ratio of 240, a tensile strength of 400 MPa, and a modulus of elasticity of 3.5 GPa. The fibers were supplied by the Chemical for Modern Building Company, Egypt.

Glass fiber (as external reinforcement):

The CMB glass fiber is characterized by its lightweight nature, non-corrosiveness, and high durability. The fibers employed in this study had an average diameter of 14 µm, a length of 12 mm, a thickness of 1 mm, and a density of approximately 2,600 kg/m^3. They exhibit a tensile strength of 1,700 MPa and a modulus of elasticity ranging from 70 to 80 GPa. These fibers exhibit an aspect ratio of 857.

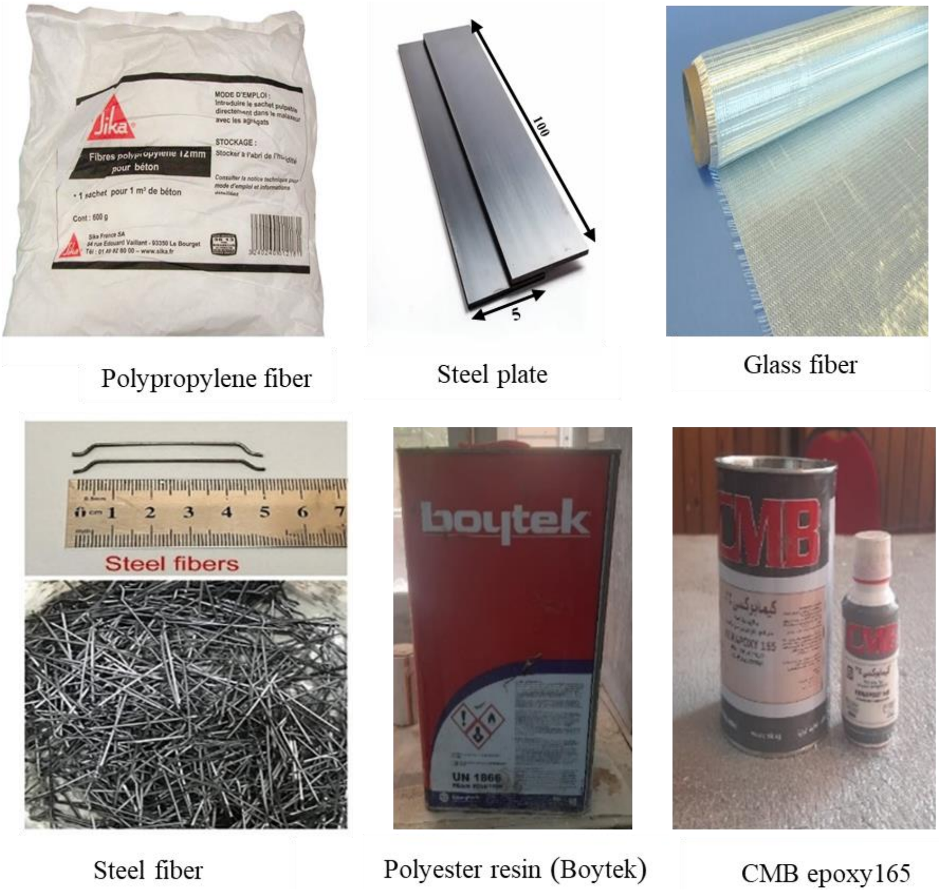

Fig. 2. Demonstration of the test materials.

3.1.7. Bacteria

Two bacterial strains were employed to induce microbial calcium carbonate precipitation (MICP) within the concrete matrix: Bacillus megaterium and strain W1. B. megaterium is a well-documented spore-forming bacterium widely recognized for its high urease activity, tolerance to alkaline environments, and compatibility with cementitious systems, whereas strain W1 was selected for its superior adaptability to harsh conditions and enhanced efficiency in calcium carbonate precipitation. Both strains are non-pathogenic, rod-shaped, Gram-positive bacteria capable of surviving the high-pH environment of concrete, as illustrated in Fig. 3. For cultivation, isolates were grown in Nutrient Broth (NB) medium containing 10 g/L peptone, 5 g/L sodium chloride (NaCl), and 10 g/L beef extract. To stimulate urease activity, the medium was supplemented with 20 g/L urea, and the pH was adjusted to 9.0–9.5 using 1 M NaOH. Cultures were incubated aerobically at 30 ± 2 °C in 2 L Erlenmeyer flasks under constant agitation at 150 rpm for 72–96 h. Growth was monitored by optical density at 600 nm (OD_{600}), and cells were harvested at OD ≈ 1.0 (≈10^8 CFU/mL), which was used as the working concentration for concrete mixing. To minimize contamination, bacterial suspensions were washed twice with sterile saline solution (0.9% NaCl) and resuspended in fresh medium immediately before use.

BM is gram-positive, spore-forming, effective at $CaCO_3$ precipitation, moderately alkali-tolerant. W1 is gram-negative, non-spore-forming, highly resistant to alkalinity and salinity, less studied but suitable for extreme conditions.

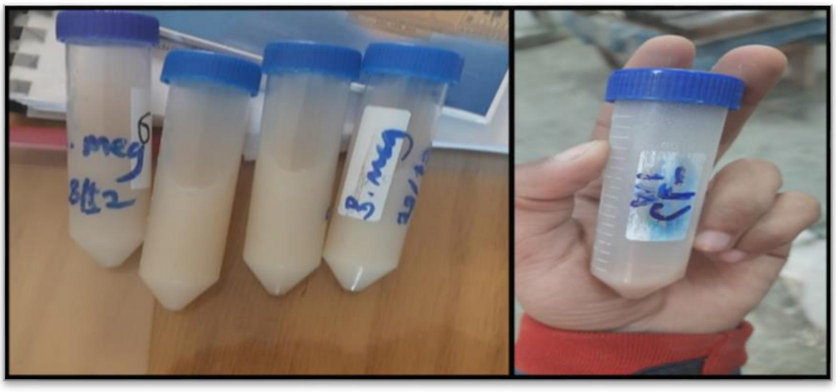

Fig. 3. Bacteria strains Bacillus megaterium and W1.

3.1.8. External reinforcement

Two types of reinforcement were used as external reinforcement for the slab samples used. Both reinforcement types were fixed on the bottom surface of the slabs (tension zone). The first type is steel plates with a thickness of 2 mm and a width of 5 cm along the slab span. Plates were fixed on the bottom surface of the slabs by using adhesive material to bond the concrete and steel plates. The adhesive used was Kima Poxy 165, which was obtained from the CMB Company in Egypt. The second type was glass fibre laminates, with the same width of steel plates (5 cm). Glass fibre laminates were fixed using polyester resin (Boytek).

3.2. Concrete mixing and mechanical testing

Concrete mixing was carried out in three successive stages. First, all dry constituents—including cement, fine aggregate, coarse aggregate, silica fume, and fibers—were blended for 2 min to ensure uniform distribution. In the second stage, 75% of the total mixing water, combined with the required dosage of superplasticizer (Sika ViscoCrete®-3425) and bacterial suspension (proportional to cement weight), was gradually added, followed by an additional 2 min of mixing. Finally, the remaining 25% of water, superplasticizer, and any residual fibers were incorporated, and mixing continued for 4 min until homogeneity was achieved. The fresh bio-concrete was cast into pre-oiled molds, compacted, demolded after 24 h, and then cured under controlled conditions until the designated testing ages. Additionally, the curing method under controlled conditions has been specified. All concrete specimens were cured at 26 ± 2 °C and 95% relative humidity for the designated curing period.

Six concrete mixes were prepared: a control mix, fiber-reinforced mixes using steel or polypropylene fibers, and bacteria-enhanced mixes using two bacterial strains (BM and W1) with and without fiber inclusion. All mixes contained a constant cement content of 500 kg/m^3, a W/C ratio of 0.42, and 10% silica fume replacement. The primary variable among the mixes was the type of fiber (steel or polypropylene) and the type of bacteria (BM or W1), added at 0.25% of cement weight. The mixed proportions are summarized in Table 4. The concrete mix proportions were designed according to ACI 211.1 (2009). The tests were conducted in accordance with ASTM C1609 (2019) using a displacement-controlled rate of 0.5 mm/min. Mechanical performance was evaluated in accordance with ES 1072/2008 (2008), ES 1658/2018 (2018), as follows:

- Compressive strength: Cubic specimens (100 × 100 × 100 mm) were tested after 7, 28, and 90 days. Reported values represent the mean of three replicates.
- Splitting tensile strength: Cylindrical specimens (100 × 200 mm) were tested after 28 and 90 days, with results averaged from three replicates.
- Flexural strength: Prismatic specimens (100 × 100 × 500 mm) were subjected to three-point bending in accordance with ASTM E399 (2020) at 28 and 90 days.
- Slab samples: Fourteen slab specimens (1000 × 500 × 50 mm with an effective span of 960 mm) were cast to evaluate structural performance. All slab, tested under four-point bending, up to failure. The slabs rested on two supports, a hinged one and a roller one. One slab was tested as a control slab. The other slabs were reinforced using two reinforcement methods: glass fiber laminates bonded with polyester resin (Boytek) and steel plates bonded with structural epoxy adhesive (CMB Epoxy 165). The reinforcing scheme is illustrated in Fig. 4. Effective span is 900 mm with simply supported boundary conditions allowing free rotation but no vertical displacement.

Table 4. Content of concrete mixes.

Mix	Cement (kg/m^3)	Water (kg/m^3)	Aggregates (kg/m^3)		Admixtures (kg/m^3)		Fiber type & dosage (volume fraction)	Bacteria type (by weight of cement)
			Coarse aggregate	Fine aggregate	Visco-Crete	Silica fume		
Control mix	500	210	1000	640	4	50	–	–
Mix 1 (ST)	500	210	1000	640	4	50	Steel fiber 0.3% (23.5 kg/m^3)	–
Mix 2 (PP)	500	210	1000	640	4	50	Polypropylene fiber 0.3% (2.7 kg/m^3)	–
Mix 3 (BMS)	500	210	1000	640	4	50	Steel fiber 0.3% (23.5 kg/m^3)	BM (0.25%)
Mix 4 (BMP)	500	210	1000	640	4	50	Polypropylene fiber 0.3% (2.7 kg/m^3)	BM (0.25%)
Mix 5 (W1S)	500	210	1000	640	4	50	Steel fiber 0.3% (23.5 kg/m^3)	W1 (0.25%)
Mix 6 (W1P)	500	210	1000	640	4	50	Polypropylene fiber 0.3% (2.7 kg/m^3)	W1 (0.25%)

Fig. 4. Glass fiber laminates and steel plate as external reinforcement.

4. Test Results

4.1. Fresh concrete properties

The flowability of fresh concrete mixes was assessed using the slump-flow spread test, and the measured values are reported in mm. Although some mixes exhibited high spread values, the concrete was not classified as self-compacting concrete (SCC). The slump-flow measurements are presented only as relative indicators of mixture flowability, and no segregation was observed during casting. The presence of high-range water-reducing admixtures (superplasticizers) and fibers can significantly influence workability. In this method, fresh concrete was placed in a cone mold, which was then lifted vertically to allow free spreading of the mix. The average spread diameter was determined by measuring in two perpendicular directions. Spread of fresh concrete is measured to indicate relative flowability. The mixes were not classified as self-compacting concrete (SCC); values are presented as indicators of workability only in Fig. 5, and the flowability results for bio-concrete mixes are summarized in Table 5.

Fig. 5. Flowability of fibrous bio-concrete.

Table 5. Flowability of bio-concrete.

Mix	Control	Mix 1 (ST)	Mix 2 (PP)	Mix 3 (BMS)	Mix 4 (BMP)	Mix 5 (W1S)	Mix 6 (W1P)
Flow (mm)	650	730	600	600	550	620	570

4.2. Hardened concrete properties

Structural performance was assessed based on slab deflection, ultimate load, and first cracking load. Compressive strength results at 7, 28, and 90 days, as well as splitting tensile and flexural strengths at 28 and 90 days, are summarized in Table 6. The mechanical properties of hardened concrete for the six investigated mixes are presented in Table 6.

Table 6. Mechanical properties of hardened concrete (MPa).

Mix	Compressive strength			Splitting tensile strength		Flexural strength	
	7 days	28 days	90 days	28 days	90 days	28 days	90 days
Control	26.67	34.33	44.67	2.34	2.44	2.67	3.55
Mix 1	33.67	46.33	58.30	2.65	2.87	3.04	4.35
Mix 2	35.00	45.00	51.33	2.61	2.65	2.70	4.35
Mix 3	33.67	49.00	51.67	2.60	2.70	3.74	4.49
Mix 4	31.00	45.33	50.00	2.65	2.76	3.21	4.94
Mix 5	42.30	52.67	58.67	2.50	2.79	3.04	4.80
Mix 6	37.67	52.00	54.00	2.44	2.90	3.31	4.82

4.2.1. Compressive strength

The compressive test setup is illustrated in Fig. 6. The average compressive strength of different mixes at 7, 28, and 90 days is shown in Fig. 7. Conventional concrete achieved strengths of 26.6, 34.3, and 44.6 MPa at these ages, respectively. All modified mixes exhibited higher values, with improvements ranging from 15% to 59% compared to the control, as follows:

- Steel fiber mix: 33.6, 46.3, and 58.3 MPa at 7, 28, and 90 days, reflecting increases of 26.3%, 34.9%, and 30.7%.
- Polypropylene fiber mix: 35, 51, and 51.3 MPa, with gains of 31.5%, 48.6%, and 15%.
- Bacillus megaterium + Steel fiber: 33.6, 49, and 51.6 MPa, corresponding to increases of 26.3%, 42.8%, and 15.6%.
- Bacillus megaterium + Polypropylene fiber: 31, 45.3, and 61 MPa, yielding improvements of 16.5%, 32%, and 36.7%.
- Bacterial W1 + Steel fiber (Mix 5): 42.3, 52.6, and 58.6 MPa, the highest overall gains of 59%, 53%, and 31%.
- Bacterial W1 + Polypropylene fiber: 37.6, 52, and 54 MPa, showing increases of 41.3%, 51.6%, and 21%.

Notably, the maximum strength of the control mix (34.3 MPa at 28 days) was matched or exceeded by bacterial–fiber concretes within just 7 days of curing, highlighting the enhanced bonding and accelerated strength development due to the fiber–bacteria interaction.

Overall, compressive strength results confirmed substantial improvements for all modified mixes. The predicted maximum load at failure closely matched the experimental ultimate load. The highest strength was obtained in Mix 5 (W1 + Steel fibers), reaching 58.67 MPa at 90 days, a 31.3% increase over the control. This enhancement is attributed to the synergistic effect of steel fibers (improved crack-bridging) and bacterial activity (calcium carbonate precipitation and densification of the microstructure).

These findings are consistent with previous studies (Helal et al. 2024; Mostofinejad et al. 2022), which reported strength gains above 37% when bacterial treatment was combined with steel fibers. Long-term studies extending to 180 days have even shown increases exceeding 45% using similar hybrid approaches.

Fig. 6. Compressive strength test.

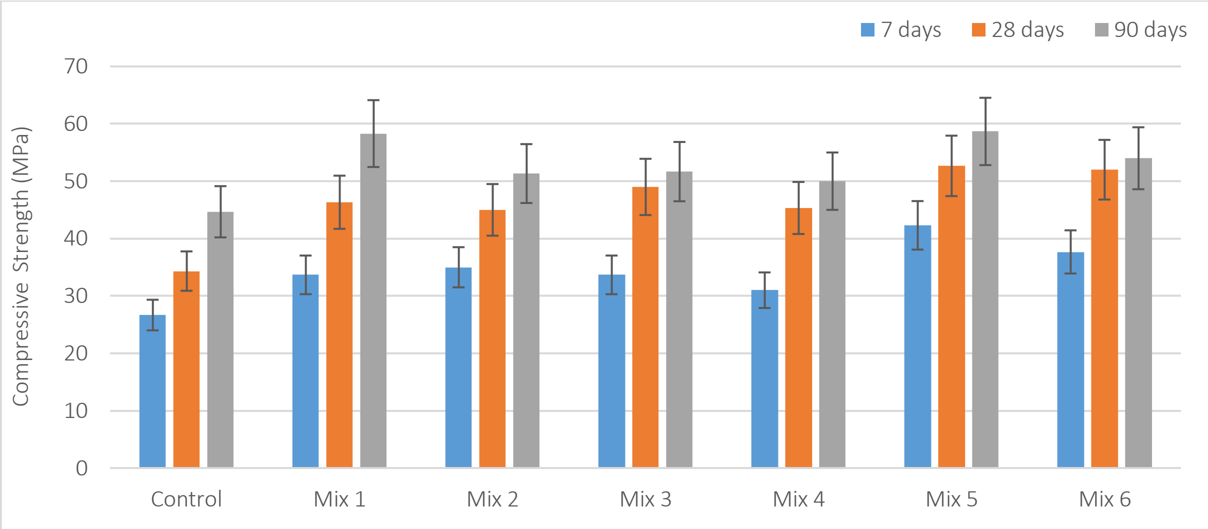

Fig. 7. The compressive strength test results.

4.2.2. Flexural strength

The loading test using the three-point loading system is illustrated in Fig.8. The mean flexural strength values of the tested mixes at 28 and 90 days are presented in Fig. 9. Conventional concrete achieved 2.66 MPa and 3.50 MPa at 28 and 90 days, respectively. All modified mixes exhibited higher values, with notable improvements depending on the type of fiber and bacterial addition, as follows:

- Steel fiber mix: 3.04 and 4.30 MPa, representing increases of 14.3% and 22.8%.
- Polypropylene fiber mix: 2.70 and 4.35 MPa, with gains of 1.5% and 24.2%.
- Bacillus megaterium + Steel fiber: 3.74 and 4.49 MPa, yielding improvements of 40% and 28.2%.
- Bacillus megaterium + Polypropylene fiber: 3.22 and 4.94 MPa, with increases of 21% and 41.1%.
- Bacterial W1 + Steel fiber: 3.04 and 5.87 MPa, the highest gain at 90 days, corresponding to 14.2% and 67.6%.
- Bacterial W1 + Polypropylene fiber: 3.31 and 4.82 MPa, showing 24.4% and 37.7% improvements.

A key observation is that the flexural strength attained by conventional concrete at 90 days was reached by bacterial fiber-reinforced concrete within 28 days, demonstrating accelerated strength development due to the synergistic effect of bacterial activity and fiber reinforcement.

Prism tests confirmed these findings, with the control mix recording 3.55 MPa at 90 days. The maximum value was observed in Mix 4 (BM + polypropylene fiber), reaching 4.94 MPa, a 39.15% increase over the control. The enhanced performance can be attributed to the combined action of fibers—which improve ductility and post-cracking load-carrying capacity—and bacterial activity, which refines the microstructure through calcium carbonate precipitation, thereby enhancing stiffness and toughness.

These results align well with previous studies (Helal et al. 2024), which reported flexural strength increases of up to 50% for bacterial concrete reinforced with steel fibers. The consistency of outcomes reinforces the evidence that microbial self-healing coupled with fiber reinforcement produces a significant synergistic effect, making bio-concrete a promising solution for durable structural applications.

Fig. 8. Flexural strength samples and test setup using a three-point loading system.

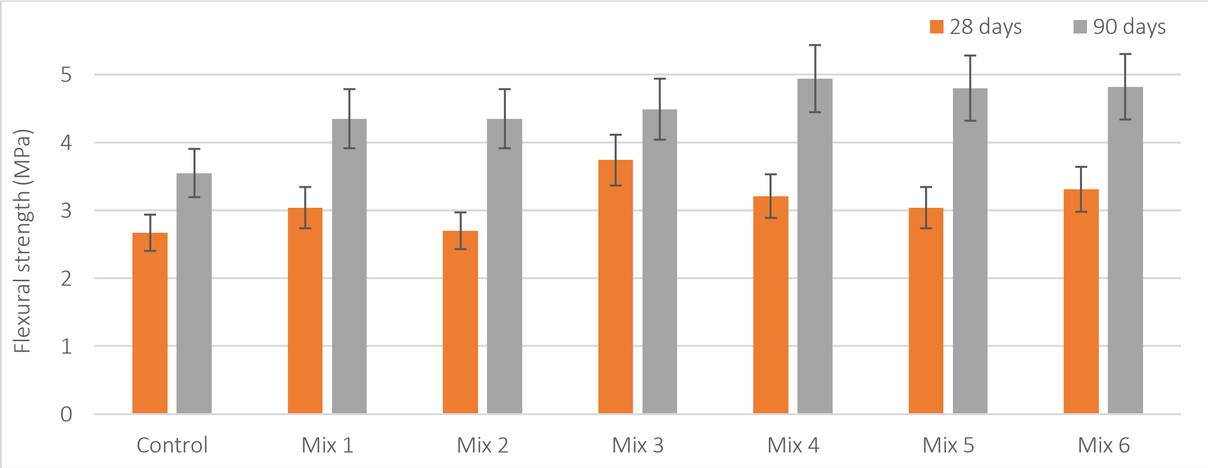

Fig. 9. The flexural strength test results.

The incorporation of fibers and bacterial strains significantly enhanced both compressive and flexural strengths of concrete, as shown in Table 7. Steel and polypropylene fibers improved load-bearing capacity and ductility by bridging microcracks, while bacterial activity (Bacillus megaterium and W1) promoted calcium carbonate precipitation, densifying the matrix and accelerating strength development.

Notably, W1-based mixes combined with steel fibers achieved the highest gains, with compressive and flexural strengths increasing up to 53% and 67.6%, respectively, and reaching conventional 90-day performance within 28 days. These results confirm a synergistic effect between fiber reinforcement and microbial self-healing, consistent with previous studies reporting 37–50% improvements under similar hybrid approaches (Helal et al. 2024; Mostofinejad et al. 2022). The findings highlight the potential of bacterial fiber-reinforced concrete for applications requiring early-age strength and enhanced durability.

Table 7. Effect of fiber reinforcement and bacterial addition on concrete mechanical properties.

Mix	Description	Compressive strength (MPa)	Increase vs. Control	Flexural strength (MPa)	Increase vs. Control
Control	Control mix	34.3 (28d)	–	3.50 (28d)	–
Mix 1	Steel fiber	46.3	34.9%	4.30	22.8%
Mix 2	Polypropylene fiber	51.0	48.6%	4.35	24.2%
Mix 3	BM + Steel fiber	49.0	42.8%	4.49	28.2%
Mix 4	BM + Polypropylene fiber	45.3	32.0%	4.94	41.1%
Mix 5	W1 + Steel fiber	52.6	53.0%	5.87	67.6%
Mix 6	W1 + Polypropylene fiber	52.0	51.6%	4.82	37.7%

4.2.3. Indirect tensile strength

The splitting tensile test setup is illustrated in Fig. 10. The mean splitting tensile strength of the tested concrete mixes at 28 and 90 days is presented in Fig. 11. Conventional concrete exhibited values of 2.34 MPa and 2.44 MPa at 28 and 90 days, respectively. All modified mixes showed improved performance, with the magnitude of increase depending on the type of fiber and bacterial addition:

- Steel fiber: 2.65 and 2.87 MPa (+13.2%, +17.6%).
- Polypropylene fiber: 2.76 and 2.65 MPa (+17.9%, +8.6%).
- Bacillus megaterium + Steel fiber: 2.60 and 2.70 MPa (+11.1%, +10.6%).
- Bacillus megaterium + Polypropylene fiber: 2.65 and 2.76 MPa (+13.2%, +13.1%).
- W1 + Steel fiber: 2.50 and 2.50 MPa (+6.8%, +2.5%).
- W1 + Polypropylene fiber: 2.44 and 2.90 MPa (+4.2%, +18.9%), achieving the highest tensile strength overall.

The results demonstrate that fiber addition enhances tensile capacity due to its inherent mechanical properties, while bacterial incorporation contributes further improvements via microbial calcium carbonate precipitation, which densifies the matrix and fills nanopores. Notably, Mix 6 (W1 + polypropylene fiber) recorded the highest 90-day splitting tensile strength of 2.90 MPa, representing an 18.8% increase over the control. Steel fiber mixes also showed substantial gains, reaching 2.87 MPa in 90 days (17.6% improvement).

These observations align with previous studies (Helal et al. 2024; Hosseinzadeh et al. 2023), where bacterial activity combined with fiber reinforcement enhanced splitting tensile strength by 17–31% over conventional concrete, confirming the synergistic effect of fibers and microbial self-healing in improving concrete tensile performance.

Fig. 10. Splitting tensile strength molds and test setup.

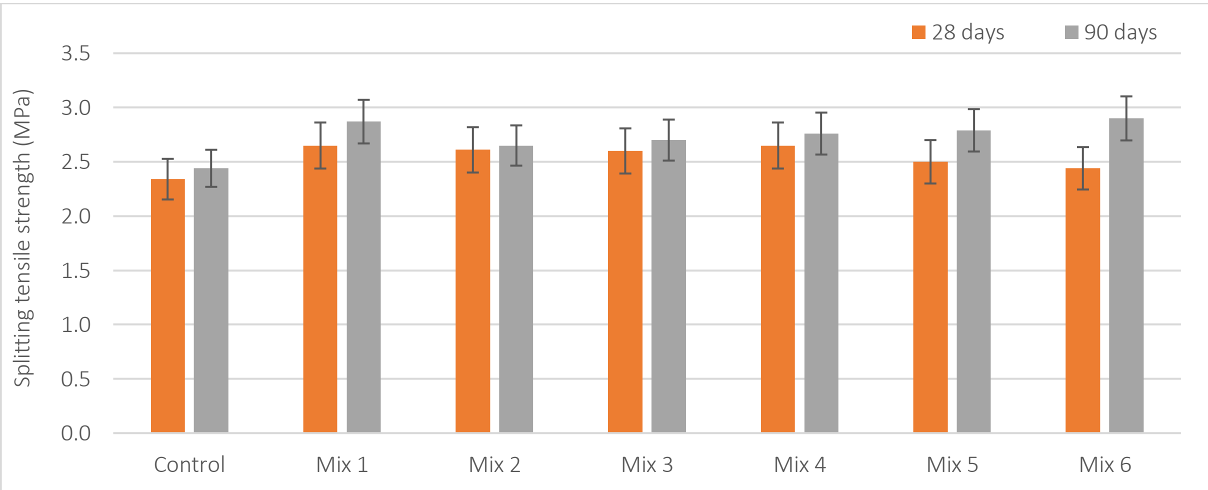

Fig. 11. Splitting tensile strength test results.

4.3. Behavior of fibrous self-healing concrete slabs

To evaluate the relative effectiveness of internal fiber reinforcement versus external reinforcement, a total of 14 concrete slabs were cast and tested under a four-point bending setup (Fig. 12). Internal reinforcement was provided by steel or polypropylene fibers incorporated into the concrete matrix, while external reinforcement involved bonding steel plates or glass fiber sheets to the slab surface. Two dial gauges were installed on each slab to measure vertical deflections at mid-span and beneath a loading point, capturing both global and localized responses. The resulting load–deflection curves (Figs. 13–15) illustrate the influence of different reinforcement strategies on stiffness, ductility, and ultimate load capacity.

The experimental results indicate that fiber-reinforced concrete slabs showed improved flexural strength and crack control compared to unreinforced control slabs, achieving higher loads before the onset of cracking. However, slabs externally strengthened with steel plates or glass fibers demonstrated significantly greater ultimate loads and reduced deflections, highlighting the effectiveness of external reinforcement in enhancing structural capacity. Notably, the combination of bacterial fiber-reinforced concrete with external reinforcement produced the highest load-bearing capacity, suggesting that internal fibers and microbial self-healing provide beneficial pre-crack microstructural improvements, which are further amplified by externally applied reinforcement.

These findings underscore the complementary roles of internal fiber reinforcement and external reinforcement: fibers enhance early-age strength, ductility, and self-healing, while external reinforcements allow substantial increases in ultimate flexural capacity, making them particularly valuable for retrofitting or strengthening applications.

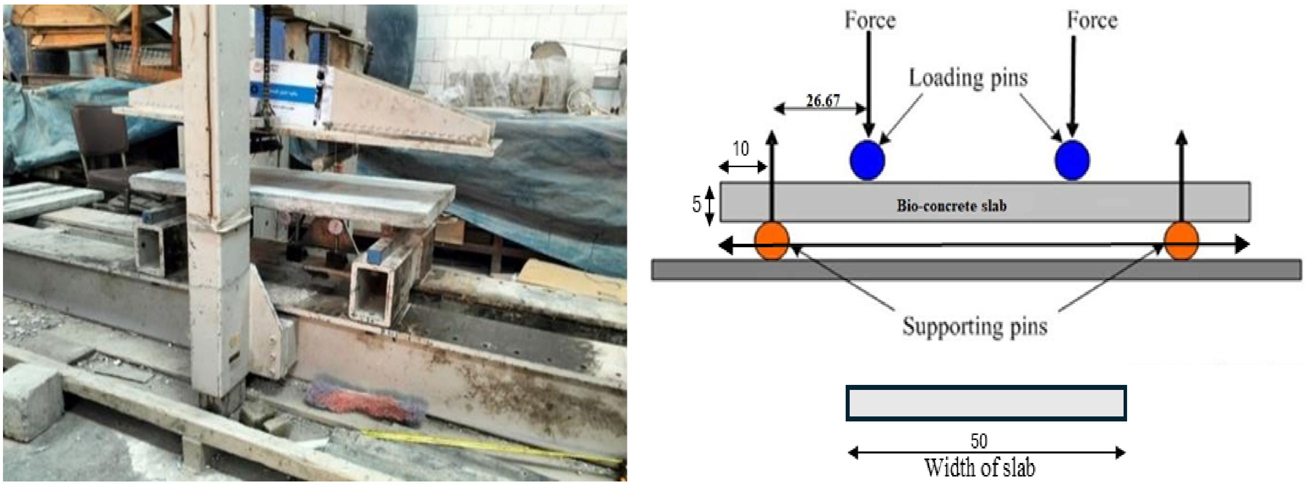

Fig. 12. Four-point loading test setup for slab samples.

Table 7 presents the experimental results for 14 slabs, including ultimate load and displacements/deflection at ultimate load. Fig. 13 shows the cracking patterns of the tested slabs, while Figs. 14 and 15 show the load-displacement curves. Each slab configuration was tested with external steel plates and glass fiber sheets to assess the influence of reinforcement on flexural performance. Across all six mixes (Table 7), slabs reinforced with steel plates consistently exhibited higher ultimate load capacities compared to those strengthened with glass fiber laminates, showing increases of approximately 15–30% over the control mix.

These results align with previous studies (İsar et al. 2023; Xie et al. 2025), which reported ultimate loads of 96.3 kN for steel-reinforced slabs versus 83.7 kN for GFRP-reinforced slabs, corresponding to a performance advantage of 15–17% in favor of steel reinforcement. The findings confirm that steel plate reinforcement provides superior flexural and impact resistance compared to GFRP-based systems, highlighting its effectiveness for structural enhancement of slabs.

Each slab configuration was tested with external steel plates and glass fiber sheets to evaluate the effect of reinforcement type on flexural behavior. Across all six mixes (Table 7), steel plate–strengthened slabs consistently demonstrated 15–30% higher ultimate load capacities than both the control and their glass fiber–strengthened counterparts. These findings are consistent with prior research (İsar et al. 2023; Xie et al. 2025), which reported ultimate loads of 96.3 kN for steel-reinforced slabs versus 83.7 kN for GFRP-reinforced slabs, a 15–17% performance advantage in favor of steel reinforcement. Overall, the results confirm that steel plate reinforcement outperforms GFRP systems in terms of flexural and impact resistance, making it a more effective technique for structural slab enhancement.

The load–deflection responses exhibited clear distinctions among the mixes. Steel fiber reinforcement (Mix 1) produced higher peak loads and pronounced ductility, whereas PP fibers (Mix 2) primarily enhanced post-cracking deformation with modest strength gains. Hybrid mixes with steel fibers and bacteria (Mixes 3 and 5) achieved the greatest improvements in ductility and load capacity, reflecting the reported synergy that elevates compressive, tensile, and flexural strengths by up to 55%, 80%, and 50%, respectively. PP fibers with bacteria (Mixes 4 and 6) also improved ductility but attained lower peak loads than their steel-fiber counterparts. Overall, the steel fiber–bacteria system provided the most effective enhancement, combining increased stiffness with superior toughness.

Each slab configuration was tested with external steel plates and glass fiber sheets to evaluate the effect of strengthening type on flexural behavior. Across all six mixes (Table 8), steel plate–strengthened slabs consistently demonstrated 15–30% higher ultimate load capacities than both the control and their glass fiber–strengthened counterparts. These findings are consistent with prior research (İsar et al. 2023; Xie et al. 2025), which reported ultimate loads of 96.3 kN for steel-reinforced slabs versus 83.7 kN for GFRP-reinforced slabs, a 15–17% performance advantage in favor of steel reinforcement. Overall, the results confirm that steel plate strengthening outperforms GFRP systems in terms of flexural and impact resistance, making it a more effective technique for structural slab enhancement.

The load–deflection responses exhibited clear distinctions among the mixes. Steel fiber reinforcement (Mix 1) produced higher peak loads and pronounced ductility, whereas PP fibers (Mix 2) primarily enhanced post-cracking deformation with modest strength gains. Hybrid mixes with steel fibers and bacteria (Mixes 3 and 5) achieved the greatest improvements in ductility and load capacity, reflecting the reported synergy that elevates compressive, tensile, and flexural strengths by up to 55%, 80%, and 50%, respectively. PP fibers with bacteria (Mixes 4 and 6) also improved ductility but attained lower peak loads than their steel-fiber counterparts. Overall, the steel fiber–bacteria system provided the most effective enhancement, combining increased stiffness with superior toughness.

It should be noted that this study does not provide direct microstructural evidence of bacterial-induced $CaCO_3$ precipitation; however, the observed improvements in mechanical properties are based on experimental observations and supported by findings from previous studies.

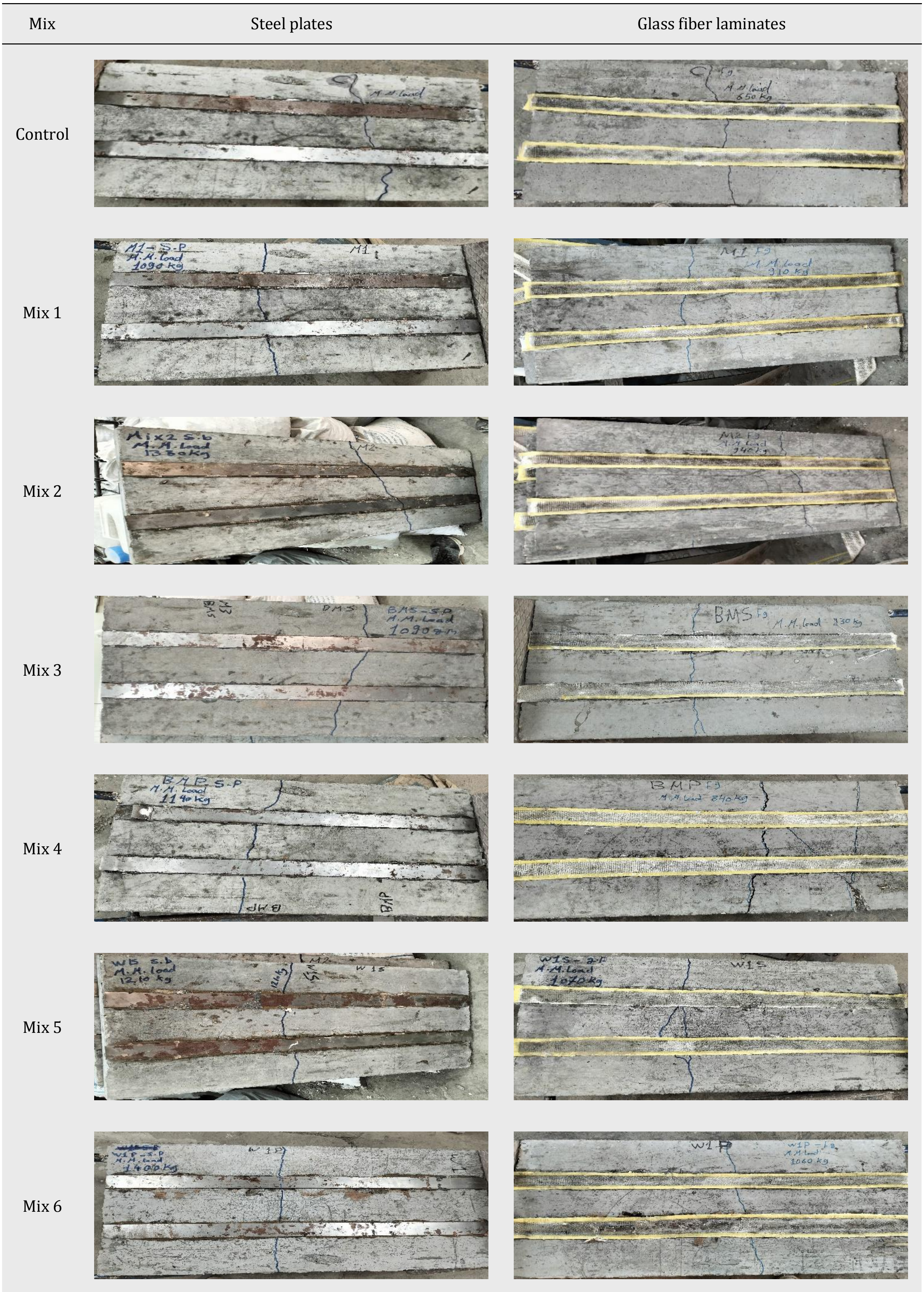

Fig. 13. Cracking pattern of investigated slabs.

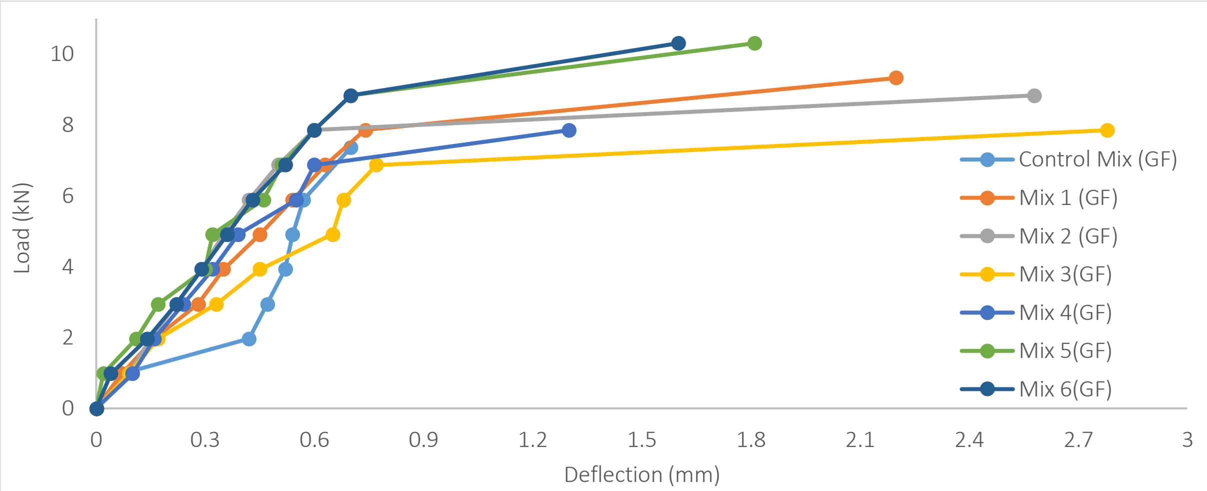

Fig. 14. Load-deflection curve when using glass fiber laminates as external reinforcement.

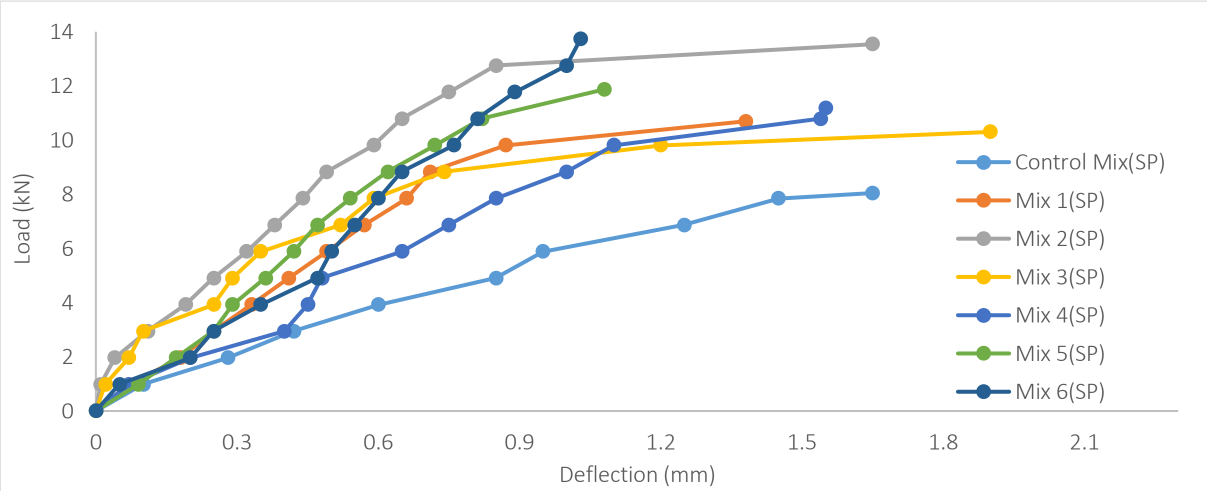

Fig. 15. Load-deflection curve when using steel plates as external reinforcement.

Table 8. Comparison between internal and external reinforcement of slabs under a four-point loading system.

Slab no.	Internal reinforcement	External reinforcement	Ultimate load (kN)	Mid-span deflection at failure (mm)	Notes
1	None (Control)	Steel plate	8.04	0.8	Baseline
2	Steel fiber	Steel plate	10.69	2.2	Improved ductility
3	Polypropylene fiber	Steel plate	13.54	2.58	Moderate improvement
4	Bacillus megaterium + Steel fiber	Steel plate	10.3	2.78	Enhanced microstructure
5	Bacillus megaterium + Polypropylene fiber	Steel plate	11.18	1.55	Moderate gain
6	W1 + Steel fiber	Steel plate	12.65	1.81	High early-age strength
7	W1 + Polypropylene fiber	Steel plate	13.74	1.03	Highest tensile gain among fibers
8	None (Control)	Glass fiber sheet	7.36	0.6	Significant ultimate load increase
9	Steel fiber	Glass fiber sheet	9.32	1.38	Synergistic improvement
10	Polypropylene fiber	Glass fiber sheet	8.83	1.65	Moderate load gain
11	Bacillus megaterium + Steel fiber	Glass fiber sheet	8.04	1.9	Moderate load gain
12	Bacillus megaterium + Polypropylene fiber	Glass fiber sheet	7.85	1.3	High ultimate load
13	W1 + Steel fiber	Glass fiber sheet	10.3	1.08	Stiffness improvement
14	W1 + Polypropylene fiber	Glass fiber sheet	10.3	0.7	Maximum ultimate load

5. Numerical Simulation

5.1. Geometry and boundary conditions

The numerical model was developed to replicate the experimental four-point bending test of reinforced concrete slabs with dimensions of 1.0 m × 0.5 m × 0.05 m. Simply supported boundary conditions were applied at both slab ends, and the load was introduced at two symmetrically placed points, each located 26.67 cm from the supports. This ensured full consistency between the experimental and numerical configurations. Fig. 16 shows the slab model in Abaqus.

5.2. Material modeling

Concrete behavior was represented using the Concrete Damaged Plasticity (CDP) model in Abaqus/CAE, which captures both tensile cracking and compressive crushing. Steel reinforcement was modeled as embedded truss elements with elastic–plastic properties, fully bonded to the concrete matrix. Material parameters for both concrete and reinforcement were derived from experimental tests to ensure accuracy.

5.3. Loading and analysis procedure

Incremental loading was applied through two concentrated forces at the same locations as in the laboratory setup. A static general analysis was performed to capture nonlinear stress–strain behavior, stiffness degradation, and crack propagation. Outputs included stress distribution, crack initiation and growth, mid-span deflection, and ultimate load capacity.

5.4. Model validation

The predicted load–deflection response and ultimate load capacity from the FE model showed close agreement with the experimental results. This confirmed that the developed model could reliably reproduce slab flexural performance and failure mechanisms. Table 9 shows a Comparison of Experimental and Numerical Results for Control and Mix 5.

5.5. Parametric analysis

To extend the experimental findings, a limited parametric analysis was carried out by comparing the control mix with Mix 5 (W1 + steel fiber + bacteria). This comparison focused on the influence of bacterial self-healing and polypropylene fibers on flexural performance. The analysis highlighted clear differences in load capacity, stiffness, and crack propagation patterns, providing insight into the synergistic contribution of microbial activity and fiber reinforcement.

5.6. Material properties

5.6.1. Concrete

The concrete used in the numerical model had a compressive strength of 35 MPa, an elastic modulus of 30 GPa, a Poisson's ratio of 0.2, a density of 2400 kg/m^3, and its stress–strain behavior was represented using the Madrid–Barbora model.

5.6.2. Steel plates

The steel plates used in the numerical model were defined using linear elastic properties with a Young's modulus of 225 GPa, Poisson's ratio of 0.25, and a density of 7850 kg/m^3.

5.6.3. Concrete stress–strain relationship

The nonlinear compressive behavior of concrete in the FE model was defined using the Madrid Parabola stress–strain relationship. This model captures both the ascending branch up to the peak compressive stress and the descending softening branch after cracking. A compressive strength of 35 MPa and peak strain 0.002 were used, with an elastic modulus calculated as $E_c = 4700\sqrt{f'c}$, and Poisson's ratio 0.2. In tension, concrete was modeled as linear elastic up to f_t = 3.2 MPa, followed by a tension-stiffening softening curve. The Concrete Damaged Plasticity (CDP) model was used with standard parameters (ψ = 35°, eccentricity = 0.1, f_{b0}/f_{c0} = 1.16, K = 0.667, viscosity = 0.0005), calibrated to match the experimental response.

The numerical model has been updated to clearly specify the element types used for each component, where concrete was modeled using 3D solid elements and steel plates using linear elastic shell/solid elements, as appropriate.

The GFRP and strengthening schemes were not included in the numerical model because the FE simulation was intended only to validate the experimental response of the control slab and Mix 5. The objective was to verify load–deflection behavior rather than simulate strengthening mechanisms.

The FEM predictions showed strong agreement with the experimental load–deflection behavior for both slabs, confirming the accuracy of the numerical modeling approach.

6. Conclusions

Based on the experiments conducted in this study to evaluate the main mechanical properties as well as the structural performance of fibrous self-healing slabs, the following conclusions can be drawn:

- Integrating bacterial self-healing agents with fibers markedly enhanced both the mechanical properties and structural performance of reinforced concrete slabs compared to the Control Mix at 90 days. The combined action of bacterial calcium carbonate precipitation and fiber crack-bridging was identified as the primary mechanism driving these improvements.
- Among the tested mixes, steel fiber–bacteria concretes achieved the highest compressive strength, with Mix 5 recording a 31.3% gain, while polypropylene fiber–bacteria concretes showed the greatest increase in splitting tensile strength, with Mix 6 achieving an 18.8% improvement.

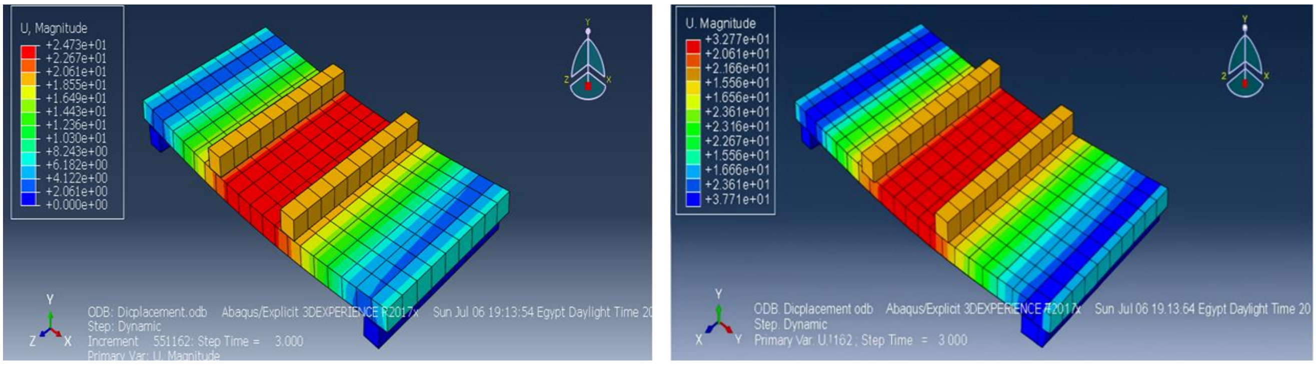

Fig. 16. Slab model simulations in Abaqus (Control Slab and Mix 5).

Table 9. Comparison between experimental and numerical results for Control Mix and Mix 6.

Mix	Ultimate load – Exp. (kN)	Ultimate load – FEM (kN)	Mid-span deflection at peak – Exp. (mm)	Mid-span deflection at peak – FEM (mm)	Stiffness trend	Remarks
Control	8.04	8.93	0.8	0.88	Lower stiffness, brittle failure	Rapid crack propagation, limited ductility
Mix 5 (W1 + SF + Bacteria)	12.65	14.22	1.03	1.12	Higher stiffness, ductile response	Enhanced crack control, delayed failure

- Flexural strength was also significantly enhanced, with Mix 4 reaching a 39.2% increase relative to the control. These findings align with previous reports that the hybrid approach of microbial self-healing and fiber reinforcement can improve concrete strength by more than 30–40% within 90 days, with potential for even greater long-term benefits.
- At the structural level, reinforcing slabs with steel plates was more effective than using glass fiber laminates, achieving gains of 15–17% and confirming the superiority of steel reinforcement. Overall, the combined use of bacteria and fibers demonstrated substantial improvements, with compressive strength enhancements reaching up to 55%, underscoring the promise of hybrid microbial–fibrous systems for high-performance, durable concrete.
- The selected mix proportions ensured adequate workability in all mixes despite fiber addition. The hardened properties showed that steel fibers enhanced compressive and flexural strength, while bacterial inclusion contributed to micro-crack healing in mixes BMS, BMP, W1S, and W1P.
- Generally, the combination of bacteria with fibers significantly boosts concrete performance, with compressive, tensile, and flexural strengths showing remarkable gains. The synergy of microbial self-healing and fiber reinforcement achieved improvements up to 55%. Steel plate reinforcing further enhanced slab behavior, offering a durable, practical, and sustainable solution for construction.

7. Recommendations

- Extend numerical simulations to include GFRP and full external strengthening schemes.
- Examine long-term durability and self-healing performance of bacterial-fiber concrete under realistic environmental conditions.
- Study the combined effects of conventional reinforcement, fibers, and bacteria on RC slab performance.
- Evaluate the influence of different bacterial species, dosages, and fiber types on mechanical properties and crack-healing behavior.

Acknowledgements

None declared.

Funding

The authors received no financial support for the research, authorship, and/or publication of this manuscript.

Conflict of Interest

The authors declare no potential conflicts of interest with respect to the research, authorship, and/or publication of this manuscript.

Data Availability

The datasets generated and/or analyzed during the current study are not publicly available but are available from the corresponding author upon reasonable request.

AI Assistance

No AI-based tools were used in the preparation of this manuscript.

Author Contributions

All authors made substantial contributions to the conception and design of the study, acquisition of data, analysis and interpretation of data; drafted or critically revised the manuscript for important intellectual content; and approved the final version to be published.

References

ACI 211.1 (2009). Standard practice for selecting proportions for normal, heavyweight, and mass concrete. American Concrete Institute, Farmington Hills, MI, USA.

Ahmed SO, Nasser AAA, Abbas RN, Kamal MM, Zahran MA, Sorour NM (2021). Production of bioconcrete with improved durability properties using alkaliphilic Egyptian bacteria. *3 Biotech*, 11(5), 231.

ASTM C1609/C1609M (2019). Standard test method for flexural performance of fiber-reinforced concrete (using beam with third-point loading). ASTM International, West Conshohocken, PA, USA.

ASTM E399 (2020). Standard test method for linear-elastic plane-strain fracture toughness of metallic materials. ASTM International, West Conshohocken, PA, USA.

Bakr MA, Hussain A, Singh PK, Singh BK, Prajakti (2024). Effects of bacterial consortium-enhanced recycled coarse aggregates on self-healing concrete immobilized with Bacillus megaterium MTCC 1684 and Bacillus subtilis NCIM 2193. *Structural Concrete*, 25(3), 1840–1864.

de Brito J, Kurda R (2021). The past and future of sustainable concrete: A critical review and new strategies on cement-based materials. *Journal of Cleaner Production*, 281, 123558.

ES 1072/2008 (2008). Egyptian standard specification for Portland cement. Egyptian Organization for Standardization and Quality, Cairo, Egypt.

ES 1658/2018 (2018). Egyptian standard specification for aggregates used in concrete. Egyptian Organization for Standardization and Quality, Cairo, Egypt.

E.S.S. 4756-1/2022 (2022). Egyptian standard specification for fiber-reinforced concrete – Part 1: Requirements. Egyptian Organization for Standardization and Quality, Cairo, Egypt.

Ganesh S, Danish P, Jessie JA, Ganie MA, Raina CS (2020). Experimental study on self-healing concrete with the effect of Bacillus subtilis bacteria to improve the strength and sustainability of the concrete. *Journal of Green Engineering*, 10(4), 1909–1923.

Griño AA, Soriano HSP, Promentilla MAB, Ongpeng JMC (2023). Exploring the potential of polypropylene fibers and bacterial co-culture in repairing and strengthening geopolymer-based construction materials. *Buildings*, 13(10), 2668.

Han S, Jang I, Choi EK, Park W, Yi C, Chung N (2020). Bacterial self-healing performance of coated expanded clay in concrete. *Journal of Environmental Engineering*, 146(7), 04020072.

Helal Z, Salim H, Ahmad SSE, Elemam H, Mohamed AIH, Elmahdy MAR (2024). Sustainable bacteria-based self-healing steel fiber reinforced concrete. *Case Studies in Construction Materials*, 20, e03389.

Hosseinzadeh H, Salehi AM, Mehraein M, Asadollahfardi G (2023). The effects of steel, polypropylene, and high-performance macro polypropylene fibers on mechanical properties and durability of high-strength concrete. *Construction and Building Materials*, 386, 131589.

Igbokwe E, Ibekwe S, Mensah P, Agu O, Abedin R (2022). Efficacy of cellulose fiber as a bacterial carrier for self-healing concrete and 3D polymer microstructure. *Proceedings for the American Society for Composites-Thirty Seventh Technical Conference*, Tucson, AZ.

Islam SU, Waseem SA (2023). Strength retrieval and microstructural characterization of Bacillus subtilis and Bacillus megaterium incorporated into plain and reinforced concrete. *Construction and Building Materials*, 404, 133331.

İsar A, Sürmelioğlu S, Andiç-Çakir Ö, Hameş EE (2023). Improvement of microstructure of cementitious composites by microbially-induced calcite precipitation. *World Journal of Microbiology and Biotechnology*, 39(3), 76.

Ji HM, Liang SM, Li XW, Chen DL (2020). Kinking and cracking behavior in nacre under stepwise compressive loading. *Materials Science and Engineering: C*, 108, 110364.

Mohammed H, Ortoneda-Pedrola M, Nakouti I, Bras A (2020). Experimental characterisation of non-encapsulated bio-based concrete with self-healing capacity. *Construction and Building Materials*, 256, 119411.

Mostofinejad D, Karimi N, Tayebani B (2022). Effect of bacterial spore in surface-treated fiber-reinforced concrete. *ACI Materials Journal*, 119, 1–12.

Mutitu DK (2019). Influence of Lysinibacillus sphaericus on compressive strength and water sorptivity in microbial cement mortar. *M.Sc. thesis*, Jomo Kenyatta University, Kenya.

Nasser AA, Esmail RF, Abbas RY, Sorour NM (2022). Effect of Bacillus megaterium bacteria and different calcium sources on strength and permeation properties of concrete. *Engineering Research Journal*, 45(3), 401–412.

Nasser AA, Sorour NM, Saafan MA, Abbas RN (2022). Microbially-induced calcite precipitation (MICP): A biotechnological approach to enhance the durability of concrete using Bacillus pasteurii and Bacillus sphaericus. *Heliyon*, 8(7), e09948.

Nimafar M, Hosseini SJ, Akhlaghi A, Samali B, Soltaninia S (2023). Effect of bacterial carbonate precipitation on the durability of concrete specimens exposed to high temperatures. *Journal of Materials in Civil Engineering*, 35(1), 04022394.

Puranik SA, Jain S, Sritam G, Sandbhor S (2019). Bacterial concrete—a sustainable solution for concrete maintenance. *International Journal of Innovative Technology and Exploring Engineering*, 8, 227–232.

Rauf M, Khaliq W, Khushnood RA, Ahmed I (2020). Comparative performance of different bacteria immobilized in natural fibers for self-healing in concrete. *Construction and Building Materials*, 259, 119788.

Rossi E, Vermeer CM, Mors R, Kleerebezem R, Copuroglu O, Jonkers HM (2021). On the applicability of a precursor derived from organic waste streams for bacteria-based self-healing concrete. *Frontiers in Built Environment*, 7, 632921.

Roy R, Rossi E, Silfwerbrand J, Jonkers H (2021). Self-healing capacity of mortars with added-in bio-plastic bacteria-based agents: Characterization and quantification through micro-scale techniques. *Construction and Building Materials*, 297, 123793.

Ryparova P, Prošek Z, Schreiberova H, Bílỳ P, Tesarek P (2021). The role of bacterially induced calcite precipitation in self-healing of cement paste. *Journal of Building Engineering*, 39, 102299.

Sadeghpour M, Baradaran M (2023). Effect of bacteria on the self-healing ability of fly ash concrete. *Construction and Building Materials*, 364, 129956.

Saridhe SP, Selvaraj T (2021). Microbial precipitation of calcium carbonate in cementitious materials–A critical review. *Materials Today: Proceedings*, 43, 1232–1240.

Singh OP, Kulhar KS, Upadhyai RP (2023). The comparison of the experimental investigations of strength characteristics of conventional and bacterial concrete. *Materials Today: Proceedings*.

Su Y, Qian C, Rui Y, Feng J (2021). Exploring the coupled mechanism of fibers and bacteria on self-healing concrete from bacterial extracellular polymeric substances (EPS). *Cement and Concrete Composites*, 120, 103896.

Su Y, Zheng T, Qian C (2021). Application potential of Bacillus megaterium encapsulated by low alkaline sulphoaluminate cement in self-healing concrete. *Construction and Building Materials*, 273, 121740.

Tang Y, Xu J (2021). Application of microbial precipitation in self-healing concrete: A review on the protection strategies for bacteria. *Construction and Building Materials*, 306, 124950.

Wachira JM, Thiong'o JK, Marangu JM, Murithi LG (2019). Physicochemical performance of Portland-rice husk ash-calcined clay-dried acetylene lime sludge cement in sulphate and chloride media. *Advances in Materials Science and Engineering*, 2019, 5618743.

Wang Y, Jiang N, Saracho AC, Doygun O, Du Y, Han X (2023). Compressibility characteristics of bio-cemented calcareous sand treated through the bio-stimulation approach. *Journal of Rock Mechanics and Geotechnical Engineering*, 15(2), 510–522.

Xie F, Tian W, Li S, Diez P, Zlotnik S, Gonzalez AG (2025). Experimental study on the structural performance of glass-fiber-reinforced concrete slabs reinforced with glass-fiber-reinforced polymer (GFRP) bars: A sustainable alternative to steel in challenging environments. *Polymers*, 17(8), 1068.

Xu J, Tang Y, Wang X (2020). A correlation study on optimum conditions of microbial precipitation and prerequisites for self-healing concrete. *Process Biochemistry*, 94, 266–272.

Zahran MA, Attia M, Nasser AA (2014). Self-healing of cracked concrete with bacterial approach. *ERJ Engineering Research Journal*, 37(2), 255-264.